Received: 16 June 2021 | Revised: 28 September 2021 | Accepted: 9 November 2021

DOI: 10.1002/2050-7038.13251

RESEARCH ARTICLE

WILEY

An improved incipient whale optimization algorithm based robust fault detection and diagnosis for sensorless brushless DC motor drive under external disturbances

Kumarasamy Vanchinathan[1] | **KarumanchettyThottam Ramasamy Valluvan[2]** | **Chinnaraj Gnanavel[3]** | **Chandrasekaran Gokul[1]** | **Johny Renoald Albert[4]**

[1]Department of Electrical and Electronics Engineering, Velalar College of Engineering and Technology, Erode, India

[2]Department of Electronics and Communication Engineering, Velalar College of Engineering and Technology, Erode, India

[3]Department of Electrical and Electronics Engineering, AMET Deemed to be University, Chennai, India

[4]Department of Electrical and Electronics Engineering, Vivekanandha College of Engineering for Women, Namakkal, India

Correspondence
K. Vanchinathan, Department of Electrical and Electronics Engineering, Velalar College of Engineering and Technology, Erode-638012, Tamilnadu, India.
Email: vanchieee@gmail.com

Handling Editor: Prof. Jalilzadeh-Hamidi, Reza

Abstract

In general, unexpected failures in sensorless brushless DC (BLDC) motors can result in production downtime, costly repairs, and safety concerns. BLDC motors are commonly used in home appliances, the medical sector, aerospace, small-scale, and large-scale industries under uncertain operating conditions. Therefore, the fault detection and diagnosis (FDD) of BLDC motor drives can play a very important role in increasing their performance, reliability, robustness control, and operational safety under uncertain operating conditions in critical real-time applications. To satisfy these issues of hall effect sensor, misplacement of a hall-effect sensor, inverter IGBT open-switch fault diagnosis, failure of hall effect sensor, lack of robustness speed control of BLDC motor, which has received substantial interest in academic and industry sectors to establish the proposed work optimization techniques approach FDD strategy for speed control of sensorless BLDC motor under uncertain operating conditions. The proposed optimization techniques such as Bat Algorithm (BA), Grey Wolf Optimization (GWO), and Whale Optimization Algorithm (WOA) approach FDD strategies for BLDC motor drives. These FDD strategies simulated by the above optimization techniques on a sensorless BLDC motor with numerical Matlab/Simulink 2020a simulation results are verified. From the simulation results, out of three optimization techniques, the WOA-based FDD strategies are very effective for both bearing and stator winding faults detection and diagnosis in sensorless BLDC motor drives.

KEYWORDS

brushless DC motor drive, fault detection, fault diagnosis, optimization techniques, sensorless speed control

List of Symbols and Abbreviations: N_s, set speed; $u(t)$, control signal; n_e, estimated speed; f_{cost1}, cost function; k, fast counter; $N(t)_{set_i}$, set speed in rad/s; $N(t)_{est_i}$, estimated speed of the BLDC motor; ω_m, angular velocity of the rotor (in rad/s); φ_a, measurement of flux; φ_g, air gap flux; T_e, electromagnetic torque; θ_r, rotor position in radian; ω_m, rotor speed in mechanical rad/s; t, indicates the current iteration; X^*, is the position vector of the best solution; AE, acoustic emission; BA, bat algorithm; BLDC, brushless DC motor; CAGR, compound annual growth rate; FDD, fault detection and diagnosis; GWO, grey wolf optimization; MCSA, motor current signature analysis; PM, permanent magnets; SF, single fault; WOA, whale optimization algorithm.

1 | INTRODUCTION

The brushless DC (BLDC) motors have become essential elements of modern production and manufacturing lines. In many applications, the motors are operated in unfavorable environments involving high temperatures and overloading.[1] These stresses together with the aging of parts may lead to motor faults. Once a failure occurs, it usually results in loss of productivity, downtime, and costly repairs. Condition monitoring leading to fault detection and diagnosis (FDD) in electric motors is therefore of a great value and has received much attention in the past few years.[2] The BLDC motor is reported for the greater sales market share in 2017, and its expected sales market growth is at 10% compound annual growth rate (CAGR) by 2026. The Figure 1 shows the electric motor expected sales market report.

Fault detection and diagnosis is a process where the condition of the equipment is monitored for signs of faults or deterioration so that maintenance or repair can be performed to prevent system failures. Instrumentation is an important consideration in FDD. Ideally, the scheme should minimize the requirement of additional sensors and use existing signals. Furthermore, it needs to avoid false positives, be reliable, and provide a clear indication of incipient faults on time. In this study, two FDD approaches were developed and implemented on a permanent magnet synchronous motor. To demonstrate their effectiveness, the FDD methods were validated by physically simulating fault conditions on a permanent magnet BLDC motor.[3] Figure 2 shows the percentage of failure of BLDC motor components.

Faults can arise in the motor rotor/motor field, stator winding/armature winding, and mechanical components of the BLDC motor. It has been shown that mechanical components cause 40% of the bearing faults, the stator winding causes 35% of the problems, the permanent magnet rotor causes 15% of the problems, and "other" defects cause the remaining 10%.[4,5]

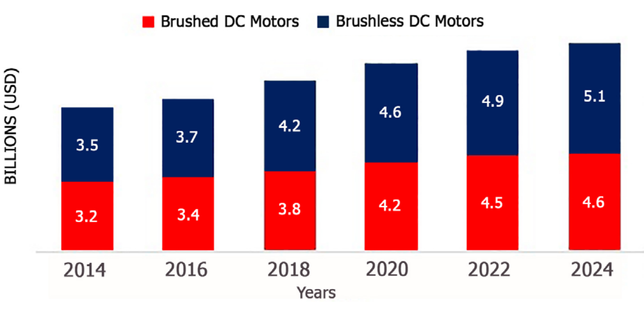

FIGURE 1 Electric motor expected sales market report. *Source*: Grand View Research

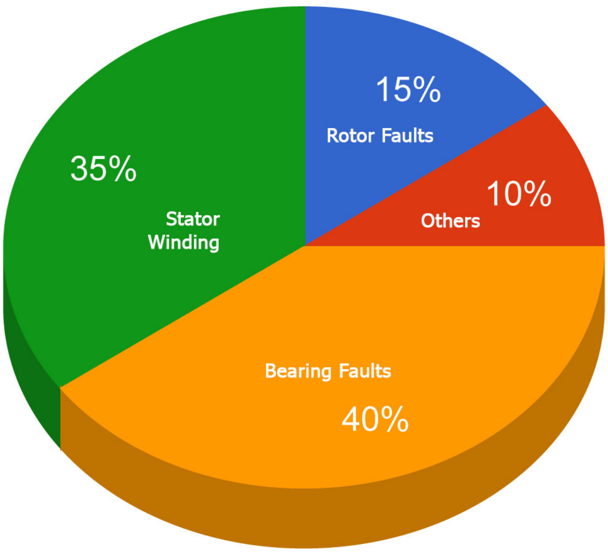

FIGURE 2 Percentage of failure of BLDC motor components

The main goal of an FDD method is to detect a fault before the performance of the machine is compromised. The absolute requirement is to detect the fault before the machine reaches catastrophic failure. In some applications, it is important to notice a fault at an early stage before they are close to compromise the performance of the machine. An example of this kind of application is the automotive industry, where performance issues will directly reduce the safety of the driver and other road users. The automotive industry also requires online FDD as well as the possibility to find fault in a disruptive environment. A disruptive environment means that signals such as mechanical torque, vibrations, and acoustics might be difficult to read due to noise.[6]

This article aims to model and simulate a faulty BLDC motor for the automotive industry. The fault should then be detected by an FDD method at an early stage. To find a suitable FDD method to predict fault with, several different methods will be considered. The most suitable FDD methods will be implemented and tested to ensure their reliability. The overall features and contributions of this study are summarized as follows:

- The bearing and stator winding issues of BLDC motor, which employs optimization approaches such as Bat Algorithm, Grey Wolf Optimization (GWO), and Whale Optimization Algorithm (WOA), dramatically improve the percentage of accuracy, robustness speed control, quick response time, reduced the percentage of fault reduction, and better transient performance of the proposed systems.
- To determine bearing fault using vibration sensor through wavelet analysis and determine stator winding fault/sensorless speed estimation using Kalman filter algorithm.

This article is organized as follows. Section 2 reviews the main literature on the fault diagnosis of electric motors, including mechanical and electrical faults. In Section 3, the methods and materials of the proposed FDD for speed control of BLDC motor are described in detail. A classification of FFD for permanent magnet BLDC motor drive based on wavelet denoising is also provided. The proposed intelligent FDD approach for speed control of sensorless BLDC motor drive using optimization techniques is presented in Section 4. In Section 5, simulation results are presented with comparisons and discussions on the performance of the proposed methods. It is shown that all simulated fault conditions were successfully detected, which demonstrates the effectiveness of the proposed methods in motor FDD with recommendations for future research. Concluding remarks are provided in Section 6.

2 | PRELIMINARY WORKS

This section focuses on the literature on FDD and their application to motors, particularly in BLDC motors. As a key component, their malfunction can harm the production line or even have severe consequences and cause heavy financial losses. For that reason, the development of FDD tools for electric motors has received much attention since the 1920s.[7] Several survey articles have been published and can be found in Reference 8. The major faults of electric motors can be broadly classified into two groups: mechanical faults such as the bearing faults, broken rotor bar, and bent shaft and electrical faults such as opening and shorting of a stator phase winding. A recent study revealed that the main causes of failure in electric motors are bearing (69%), stator windings (21%), rotor bar (7%), and shaft/coupling (3%).[9] The various types of fault in the BLDC motor are shown in Figure 3.

The bearing failure mechanism has been studied for almost four decades.[10] As such, the theoretical foundation of bearing failure modes has been considered comprehensively.[11] While there are monitoring techniques based on different measurement sources, such as acoustic emission (AE) and motor current signature analysis (MCSA), vibration monitoring is probably the most widely used approach.

Vibration in an electric motor can come from many sources including bearings, electromagnetic forces, unbalanced rotors, etc. Each will have its signature in the frequency domain that can manifest itself as discrete frequency bands. To extract fault signatures buried in vibration signals from the machine, advanced signal processing techniques are commonly used. These include filtering and feature extraction of the vibration data.[12]

In the analysis of vibration measurement, signal modulation effect and noise are two major barriers in detecting the presence of bearing faults at early stages. Due to the amplitude-modulated effect, the BPFs usually appear as sidebands of resonance frequency in the spectrum. This makes identifying the specific frequency components difficult. Thus, an effective signal demodulation technique should be used. Meanwhile, weak signatures produced by incipient bearing faults can easily be masked by noise in a real environment, making fault detection even more difficult. Hence, a

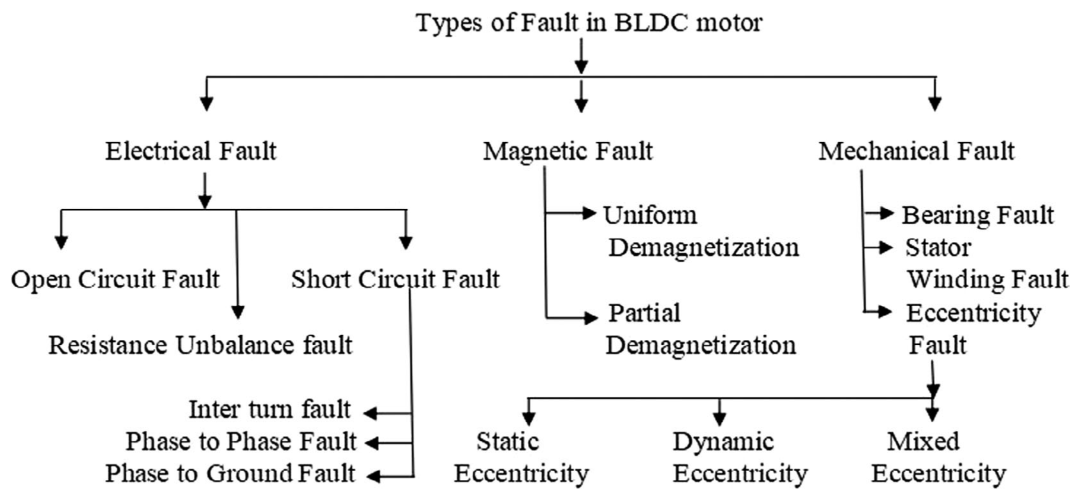

FIGURE 3 Types of fault in BLDC motor

denoising algorithm is also necessary to enhance the extraction of characteristic features of bearing faults. To overcome these barriers, numerous studies have been conducted on signal processing techniques for bearing diagnosis.[13,14]

During electrical fault in BLDC motors, the permanent magnets replace the rotor windings, thus the electrical faults are mostly stator-related. Two mains classes of stator winding fault are: (a) the open-phase fault and (b) the shorted turns or the turn-to-turn insulation fault. The former may allow the machine to operate with reduced torque, while the latter can quickly develop into an insulation failure and the complete breakdown of the machine. An insulation failure normally starts with an interturn short circuit, which induces a high current and much heat that burns the insulation. If left undetected, turn-to-turn faults will propagate to the stator core and lead to phase–phase or phase–ground failure.[15] This failure can occur within 60 seconds for small low-voltage motors and usually lead to irreversible damage to the machine.

Condition monitoring and fault diagnosis of electric motors are important features that can improve the reliability of industrial machinery. In general mechanical faults and electrical faults of electric motors, with a special focus on bearing and stator winding faults. In terms of bearing faults, vibration-based techniques are the most reliable.[16] To enhance the characteristic features of a fault, several signal processing techniques have been proposed. Among them, the wavelet analysis has shown its superiority in signal denoising and feature extraction. In terms of stator winding faults, the model-based parameter estimation techniques were found to be most promising. These methods are nonintrusive and can track the variation of actual physical parameters. Most of the reviewed literature, however, only considers the bearing faults or the stator winding faults exclusively.[17]

A combined strategy that can handle both of these faults would be more capable for practical use. Besides, for the wavelet-based methods applied on bearing diagnosis, the merits of complex wavelet transform in improving the signal denoising performance are not fully exploited. Moreover, the influence of modeling uncertainties on the parameter estimation of electric motors should be considered to provide a robust fault diagnosis scheme.[18] Accordingly, FDD strategy based on wavelet analysis and robust state estimation techniques was proposed in this article; the implementation of the proposed methods on a BLDC motor was also investigated. Details of the proposed strategy and its implementation will be discussed in the following sections.

2.1 | Formula for the cost function

The sampling frequency is defined as $f_{sample} = 1/\text{sample}$, which functions as a fast counter k in this example. The commutation interval can be "counted" by the fast counter k, which is reset at each change of the Hall sensor state, yielding the saw-tooth curves. The time interval from the last commutation instant can be computed using this fast counter k as follows:

$$f_{\text{cost 1}} = \boldsymbol{\tau} = \boldsymbol{k}.\boldsymbol{\tau}_{\textbf{sample}}. \tag{1}$$

The setting a threshold for the value of is important for diagnosing abnormal circumstances. This limit is defined in relation to the predicted or average value, which may be determined using the preceding 180 electrical degrees as

$$f_{\text{cost 1}} = \boldsymbol{\tau_n} = \frac{\mathbf{1}}{\mathbf{3}}\sum_{\boldsymbol{i}=\mathbf{1}}^{\mathbf{3}} \boldsymbol{\tau}(\boldsymbol{n}-\boldsymbol{i}). \tag{2}$$

After the single defect has been identified, the average value of commutation intervals should be adjusted to maintain the BLDC motor drive's FFD. When a single defect occurs, one of the Hall sensors' transitions evaporates, leaving only two commutation intervals for 180 electrical degrees. As a result, (3) can be changed to n, with the superscript "SF" denoting a single fault.

$$f_{\text{cost 1}} = \boldsymbol{\tau_n}^{\boldsymbol{SF}} = \frac{\mathbf{1}}{\mathbf{3}}\sum_{\boldsymbol{i}=\mathbf{1}}^{\mathbf{2}} \boldsymbol{\tau}(\boldsymbol{n}-\boldsymbol{i}). \tag{3}$$

T_m equals T_0 in a steady-state operation, hence Equation (4) can be reduced to:

$$\omega_r = \frac{1}{\mathrm{J}}\int -T_c\cos\,(\omega_c t)dt = \omega_{ro} - \frac{T_c}{J\omega_c}\sin(\omega_c t), \tag{4}$$

$$t = \frac{1}{\frac{P}{2}(6*\omega_{\text{ref}})}, \tag{5}$$

$$\omega_h = 6*\frac{5}{\rho*\Delta T_x}, \tag{6}$$

$$\omega_{\text{sect}} = \frac{5}{\rho*\Delta T_y}. \tag{7}$$

3 | METHODS AND MATERIALS

Methods and materials of the proposed FDD strategy of sensorless approach speed control of BLDC motors are studied in this section. As well as the formation of objective functions, bearing faults, stator winding fault, electrical faults, vibration, and noise estimation of sensorless BLDC motors are discussed. The fault taxonomy of BLDC motor derives is shown in Figure 4.

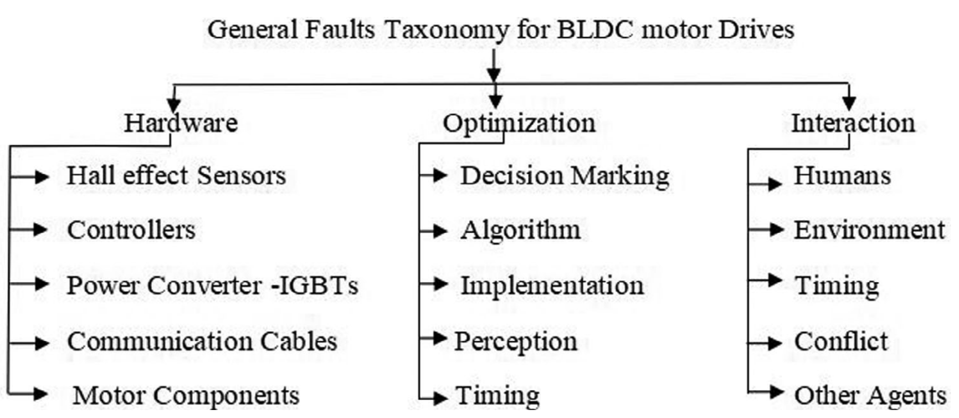

FIGURE 4 Fault taxonomy for BLDC motor drives

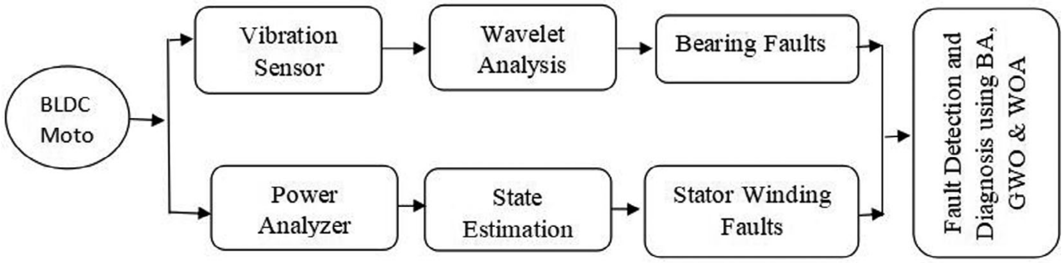

FIGURE 5 Proposed fault detection and diagnosis scheme for BLDC motor

3.1 | Formation of objective functions

- The objective of this research has been to develop optimization techniques (a) BA-, (b) GWO-, (c) and WOA-based FDD strategy for sensorless BLDC motor bearing faults and motor winding faults at their inception.
- These bearing and motor winding faults were numerically simulated on a sensorless BLDC motor using matrix laboratory 2020a.
- The FDD strategies involving wavelets and state estimation were successfully implemented. Numerical simulation results are confirmed that the proposed optimization techniques based FDD schemes were very effective in detecting bearing and winding faults in BLDC motors. The proposed FDD scheme for the BLDC motor is shown in Figure 5.

3.2 | Bearing fault of BLDC motor

Rolling bearings of various kinds are widely used in industrial machines. They provide fundamental mechanical support for rotating parts. Most rotating shafts use a rolling element bearing. To ensure the effectiveness and robustness of these bearings, their performance under various and extremely demanding conditions has been extensively studied.[19] While there are various kinds of rolling bearings in the market, their associated fault detection approaches are analogous. Therefore, one of the most commonly used types of bearings, the single-row deep-groove radial ball bearing, is selected in this research. These bearings consist of an inner ring, an outer ring, rolling elements (balls), and a cage (retainer). The inner ring has a groove on its outside diameter with a smooth finishing surface and extremely tight tolerances to form a path for the balls.

The inner ring is mounted on the shaft of the motor and rotates with the shaft at the same speed. The outer ring is the counterpart of the inner ring and has a groove on its inside diameter with a high precision finish. The outer ring is placed into the housing on the motor case and thus held stationary concerning the motor. The rolling balls are located between the inner ring and outer ring. These balls have slightly smaller diameters than the grooved ball track, which allows them to contact the rings at a single point.[20] This point contact enables the bearing to rotate with minimal friction. To achieve point contact, the tolerances are strictly controlled to a micro inch level, as well as the dimensions of the balls and rings. Accordingly, the performance of a bearing is closely related to the critical surfaces, particularly those entering the load zone at a given time.[21] The structure of the ball bearing in the BLDC motor is shown in Figure 6.

3.3 | Stator winding fault

The control of a BLDC motor has become easy and reliable, allowing the motor to be operated over a wide range of speeds with ease. It has several advantages, including excellent speed-torque characteristics, decent static and dynamic characteristics, high performance, higher speed ranges up to 10 000 rpm, long service life, and quiet operation. The stator winding of the BLDC motor is made of stacked laminated steel.[22] There are two types of connections: star relation and delta. The star connection provides high starting torque at slow speeds, while the delta connection provides low starting torques at slow speeds. The BLDC motors can run on single-phase, two-phase, or three-phase alternating currents. The three-phase BLDC motor is well-known and widely used.[23]

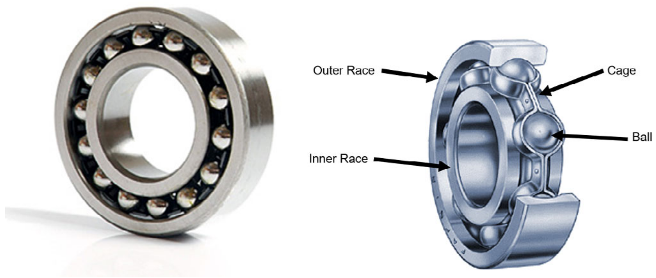

FIGURE 6 Structure of ball bearing in BLDC motor

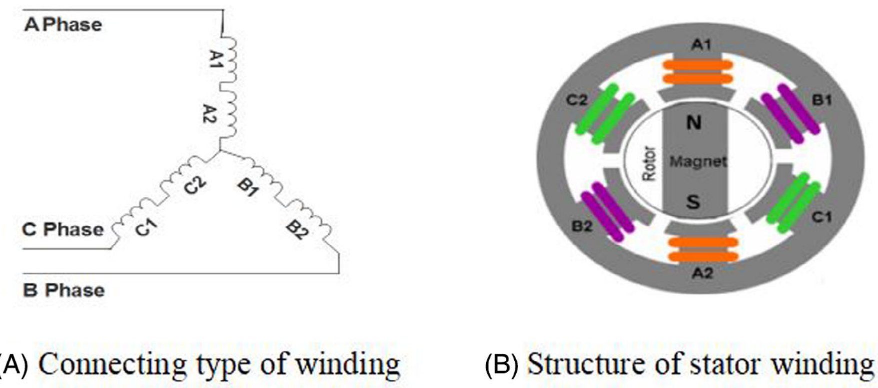

FIGURE 7 Schematic diagram of the stator winding in BLDC motor. (A) Connecting type of winding. (B) Structure of stator winding

The rotor parts are made of permanent magnets (PM), which are composite or ferrite magnets that can be used in 2 to 8 PM pole arrangements with the north pole and the south pole alternating. The magnetic flux interaction in the rotor varies depending on the magnetic material used. The best magnetic material available increases performance. The majority of rotors used recently are rare earth alloy PM. Figure 7 depicts the schematic diagram of the stator winding in the BLDC motor.

Furthermore, these alloy magnets improve the size-weight ratio and provide more torque for the same size. The BLDC motor's commutation is operated electronically using an electronic commutator. The stator windings A1A2, B1B2, and C1C2 must be energized to operate the BLDC motor. Sensors and sensing elements installed into the stator winding side at 120° displacement are used to detect the location of the PM rotor. Knowing the location of the PM rotor using Hall Effect sensors to determine the stator winding (A1A2, B1B2, and C1C2) would be energized first.

3.4 | Electrical faults

For BLDC motors, the permanent magnets replace the rotor windings, thus the electrical faults are mostly stator-related. Two mains classes of stator winding fault are: (a) the open-phase fault and (b) the shorted turns or the turn-to-turn insulation fault. The former may allow the machine to operate with reduced torque, while the latter can quickly develop into an insulation failure and the complete breakdown of the machine. An insulation failure normally starts with an interturn short circuit, which induces a high current and much heat that burns the insulation. If left undetected, turn-to-turn faults will propagate to the stator core and lead to phase-phase or phase-ground failure. This failure can occur within 60 seconds for small low-voltage motors and usually lead to irreversible damage to the machine.[24]

3.5 | Vibration and speed estimation using kalman filter

A Kalman filter evaluates the past estimate and the most current input data to create new estimate data using the recursive approach. As a consequence, the filter just needs to save the previous estimate and may fit the real-time requirements of the system.[25] Furthermore, the Kalman filter is a computer-implemented recursive method. The vibration and rotor speed of the BLDC motor are determined by using the Kalman filter.

The control strategy of a Kalman filter based on line back—EMF and the terminal voltage model of the BLDC motor as

$$\begin{cases} e_{AB} = u_{AG} - u_{BG} - (\mathrm{L}-\mathrm{M})\dfrac{d(i_{A-}i_B)}{dt} - \mathrm{R}(i_{A-}i_B) \\ e_{AC} = u_{AG} - u_{CG} - (\mathrm{L}-\mathrm{M})\dfrac{d(i_{A-}i_C)}{dt} - \mathrm{R}(i_{A-}i_C), \\ e_{BC} = u_{BG} - u_{CG} - (\mathrm{L}-\mathrm{M})\dfrac{d(i_{B-}i_C)}{dt} - \mathrm{R}(i_{B-}i_C) \end{cases} \tag{8}$$

$$e_{BC} = e_{AC} - e_{AB}. \tag{9}$$

The voltage model is simplified as

$$U_1 = \begin{bmatrix} 2\left(R + \dfrac{d}{dt}(L-M)\right) & 0 \\ R + \dfrac{d}{dt}(L-M) & 3\left(R + \dfrac{d}{dt}(L-M)\right) \end{bmatrix} I_1 + E_1. \tag{10}$$

State model is established as

$$X_{k+1} = \Phi_k K_k + R_k U_k + G_k\, w(k), \tag{11}$$

$$y_k = H_k X_k + v(k), \tag{12}$$

where,

$$X_k = [i_{AB}(k)\, i_{AC}(k)\, e_{AB}(k)\, e_{AC}(k)\, \omega(k)]^T, \tag{13}$$

$$R_k = \begin{bmatrix} \dfrac{T}{2(L-M)} & -\dfrac{T}{6(L-M)} & 0 & 0 & 0 \\ 0 & \dfrac{T}{3(L-M)} & 0 & 0 & 0 \end{bmatrix}^T, \tag{14}$$

$$U_k = [u_{AB}(k)\, u_{AC}(k)]^T, \tag{15}$$

$$y_k = [i_{AB}(k)\, i_{AC}(k)]^T, \tag{16}$$

$$\Phi_k = \begin{bmatrix} 1 - \dfrac{RT}{L-M} & 0 & -\dfrac{T}{2(L-M)} & 0 & 0 \\ 0 & 1 - \dfrac{RT}{L-M} & \dfrac{T}{6(L-M)} & -\dfrac{T}{3(L-M)} & 0 \\ 0 & 0 & 1 & 0 & 0 \\ 0 & 0 & 0 & 1 & 0 \\ 0 & 0 & 0 & 0 & 1 \end{bmatrix}, \tag{17}$$

$$H_k = \begin{bmatrix} 1 & 0 & 0 & 0 & 0 \\ 0 & 1 & 0 & 0 & 0 \end{bmatrix}, \tag{18}$$

where,

t_{k+1}—state equation and estimation error covariance matrices.

t_k—state equation and inputs at time.

The state equation is

$$\widehat{X}_{K+1\,|\,K} = \Phi_k \widehat{X}_{K\,|\,K-1} + K_k\left(y_k - H_k \widehat{X}_{K\,|\,K-1}\right) \tag{19}$$

$$= (\Phi_k - K_k H_k)\widehat{X}_{K\,|\,K-1} + K_k y_k. \tag{20}$$

In which,

$$K_k = \Phi_k P_{k|k-1} H_K^T \left(H_k P_{k|k-1} H_k^T + R_k\right)^{-1}. \tag{21}$$

The estimation error covariance matrix prediction equation is,

$$P_{k+1|k} = \Phi_k\left[P_{k|k-1} - P_{k|k-1}H_k^T\left(H_k P_{k|k-1} H_k^T + R_k\right)^{-1} H_k P_{k|k-1}\right]\Phi_K^T + \qquad G_k Q G_k^T. \tag{22}$$

The estimation and the error covariance can be updated by

$$\widehat{X}_{K\,|\,K} = \widehat{X}_{K\,|\,K-1} + P_{k|k-1}H_k^T\left(H_k P_{k|k-1} H_k^T + R_k\right)^{-1}\left(y_k - H_k \widehat{X}_{K\,|\,K-1}\right), \tag{23}$$

$$P_{k|k} = P_{k|k-1} - P_{k|k-1}H_k^T\left(H_k P_{k|k-1} H_k^T + R_k\right)^{-1} H_k P_{k|k-1}, \tag{24}$$

Thus, based on the line back-EMF and vibration estimated by a Kalman filter, a novel commutation strategy is obtained.

4 | FDD-BASED SPEED CONTROL OF SENSORLESS BLDC MOTOR DRIVE USING OPTIMIZATION TECHNIQUES

This section firstly presents the various categories of fault in BLDC motor and proposed FDD for speed control of sensorless BLDC motor drive are discussed. Secondly, the FDD methods to implement in BLDC motor drives are presented in detail and thoroughly discussed. Figure 8 shows the taxonomy of FDD.

4.1 | Optimization algorithms

The BA or bat-inspired algorithm was introduced by Yang,[17] and GWO is an optimization algorithm is developed by Mirjalili.[18] The GWO imitates the hierarchy hunting leadership of grey wolves for survival in nature. Grey wolves are naturally a powerful predator of prey, and it has a characteristic to live in a group size of 5 to 12 wolves.

Seyedali Mirjalili and Andrew Lewis proposed important optimization techniques, namely WOA.[19,20] It is a similar procedure for the hunting behavior of whales[21] that identifies the finest search agent to chase the prey and uses a spirally simulated. The humpback whale can detect the distance and surrounding coverage location with the desired target. It is noted that humpback whale able to migrate up a coiled track at a depth of about 15 m with the diverse size of bubbles. It covers the desired target tightly with a massive spider-knotted web and makes the desired target toward the middle of the coverage location.[22,23]

The optimal search as shown in Equations (17) and (18)

$$D = |C.\, X^*(t) - X(t)|, \tag{25}$$

$$X(t+1) = X^*(t) - A.D. \tag{26}$$

The paths A and C are considered as follows

$$A = 2a.r.a, \tag{27}$$

$$C = 2.r. \tag{28}$$

Humpback is created as shown in the following equation

$$X(t+1) = D'.e^{bl}.\cos(2\pi l) + X^*(t). \tag{29}$$

Keep informed of the position as follow

$$X(t+1) = \begin{cases} X^*(t) - A.D & if\ p \leq 0.5 \\ D'.e^{bl}.\ \cos(2\pi l) + X^*(t) & if\ p \geq 0.5 \end{cases}. \tag{30}$$

The equation of the exploration phase as follows

$$D = |C.X_{rand} - X|, \tag{31}$$

$$X(t+1) = X_{rand} - A.D, \tag{32}$$

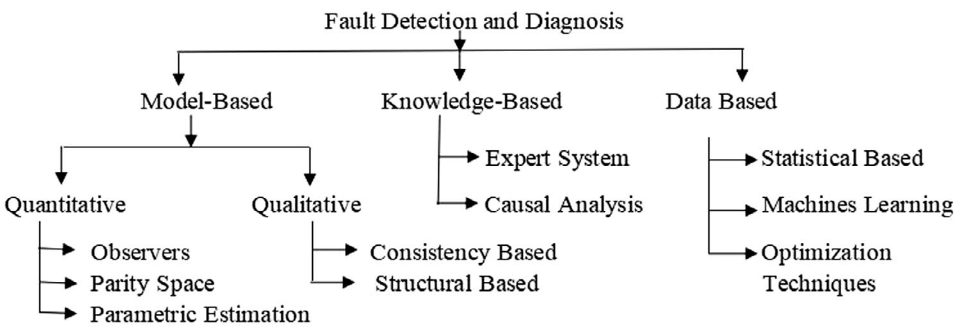

FIGURE 8 Taxonomy of fault detection and diagnosis

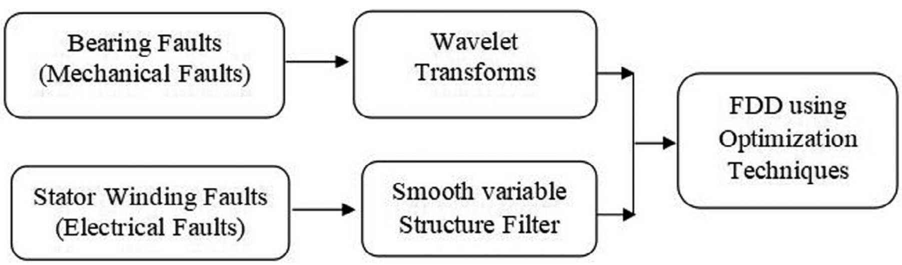

FIGURE 9 Bearing and stator winding of fault detection and diagnosis

where, t is the current iteration, X^* is the position vector, X indicates the position vector of a solution, r is random vector, A is a random value, b is a constant, p is a random number, X_{rand} is a random position path, and A and C are coefficient paths.

4.2 | Bearing fault diagnosis using wavelet transforms

The signal denoising methods based on wavelet shrinkage and Dual-Tree Complex Wavelet Transform are described. Moreover, the kurtosis and the envelope analysis are introduced, both of which are essential tools in bearing fault

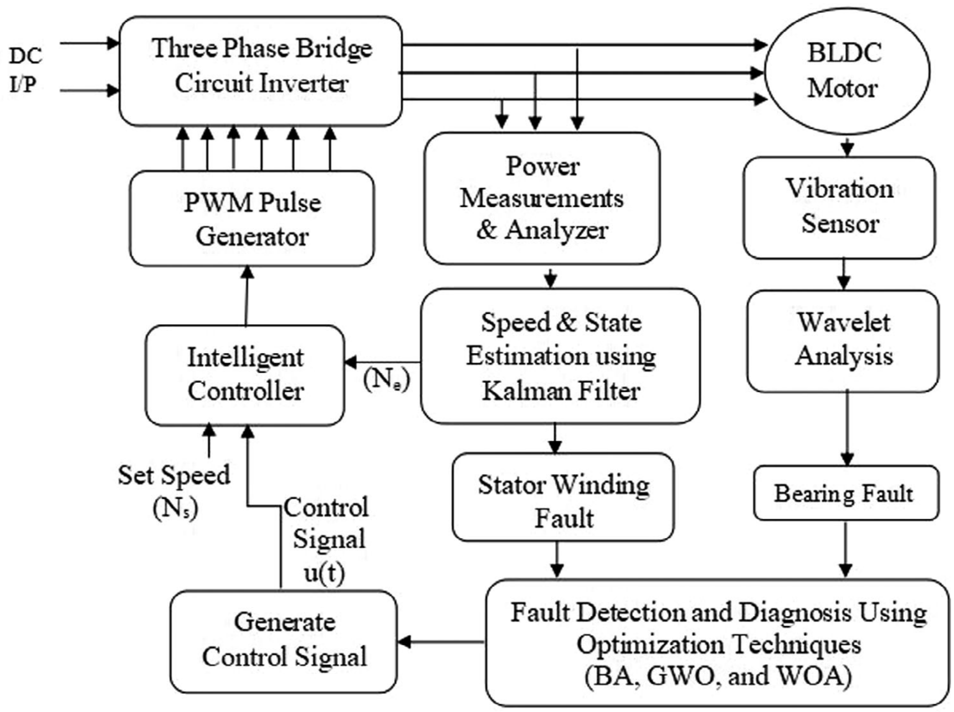

FIGURE 10 Functional blocks of optimization techniques–based FDD for speed control scheme of BLDC Motor Drive

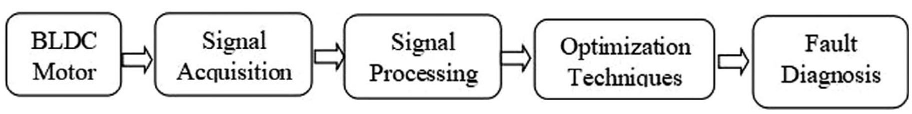

FIGURE 11 Representation of knowledge-based fault diagnosis

TABLE 1 Parameters of optimization algorithm

Bat algorithm (BA)		Grey wolf optimization (GWO)		Whale optimization algorithm (WOA)	
Population size (Xi)	10	Population	10	Population size (Xi)	10
No of dimension	3	S. diffusion	2	Random vector	0; 1
Number of iteration	10	Number of iterations	10	Number of Iterations	10
Loudness (A)	90	Lower bounds	[0.001 0.001 0.001]	Random number (p)	−1; +1
Pulse rate (R)	[1, 10]	Upper bounds	[20 20 20]	Reference whale	>1 or <1
Changing frequency	1-90 kHz	Random walk	0.75	Probability percentage	50%
Echolocation	8-10 ms	-	-	-	-
Wavelength	2-14 mm	-	-	-	-

TABLE 2 Bearing and BLDC motor parameters

Bearing parameters	Values	BLDC motor parameters	Values
Model number (N.O)	6207NSE	Rated speed (ω_r)	3000 rpm
Outer diameter (D)	72 mm	Number of poles (P)	8
Inner diameter (d)	35 mm	Moment of inertia (J)	4.8×10^{-3} kgm^2
Width (B)	17 mm	Torque constant (Kr)	1.52 Nm/A
Number of rolling balls (N_b)	11	Voltage constant (Ke)	0.77 V/(rad/s)
Contact angle (θ)	0°	Winding resistance (R)	4.8×10^{-3} H

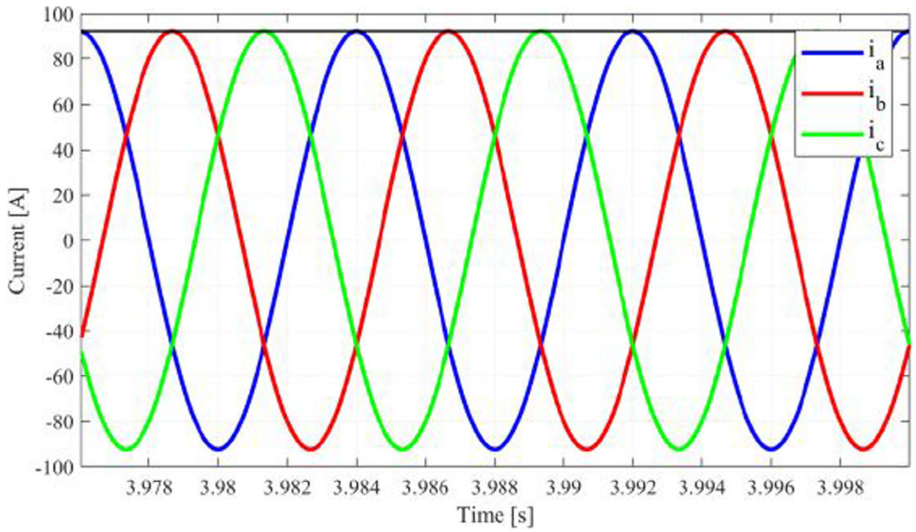

FIGURE 12 shows the three-phase currents

diagnosis.[26] The implementation of these tools on the fault diagnosis of bearings is discussed. The bearing and stator winding faults of FDD using optimization techniques are shown in Figure 9.

4.3 | Proposed FDD for speed control of sensorless BLDC motor drive using optimization techniques

The optimization techniques approach FDD for speed control of sensorless BLDC motor are mainly focused on two important faults; (a) bearing faults and (b) stator winding faults. The ball or rolling element bearings are used in the majority of electrical equipment. Each bearing is made up of two rings: an inner and an outer ring. Inside these rings, a set of balls or rolling components are positioned in raceways and revolve. The mechanical stress failures can occur even under normal operating circumstances with a balanced load and acceptable alignment. Bearing flaking or spilling can occur when minor components of the bearing come off due to mechanical stress. Other sources of bearing failure include vibration, intrinsic eccentricity, and bearing currents, in addition to regular internal working loads.[27]

The switching timing is determined by the switching logic. In the sensorless technique, voltage and current values are measured, and the actual rotor speed is estimated by the Kalman filter algorithm.[28] Figure 10 shows the functional blocks of the FDD for sensorless speed control of the BLDC motor.

The WOA approach is used for the following two purposes: (a) To reduce the error value(s) between given set speed (N_s) and obtained estimated speed (N_e) from system models. A variety of diagnostic procedures have been developed to date to diagnose BLDC motor defects.

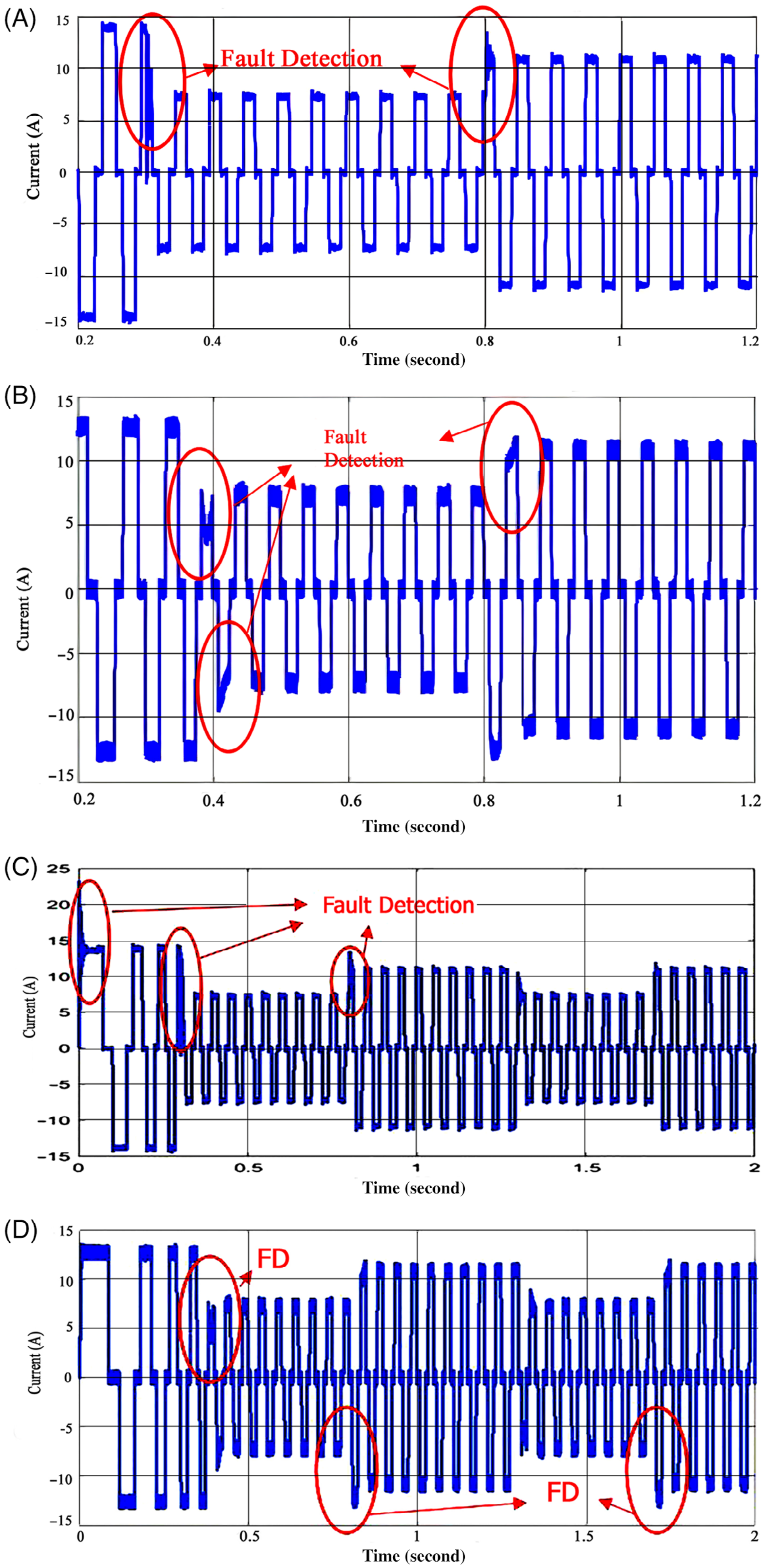

FIGURE 13 (A) Fault detection for stator current in stator winding of BLDC motor. (B) Fault detection for stator current in stator winding of BLDC motor. (C) Fault detection for stator current in stator winding of BLDC motor. (D) Fault detection for stator current in stator winding of BLDC motor

TABLE 3 Simulation test results under variable speed conditions

S. No	Operating conditions	Optimization techniques	Number of misclassifications	Maximum misclassification time (s)	Response time (s)
1	500 rpm, variable load	BA-FDD	2	0.08	0.20
		GWO-FDD	2	0.13	0.28
		WOA-FDD	1	0.06	0.30
2	1000 rpm, variable load	BA-FDD	3	0.52	0.36
		GWO-FDD	1	0.43	0.36
		WOA-FDD	1	0.28	0.42
3	1500 rpm, variable load	BA-FDD	3	0.64	0.55
		GWO-FDD	2	0.51	055
		WOA-FDD	1	0.43	0.67
4	2000 rpm, variable load	BA-FDD	2	0.79	0.64
		GWO-FDD	2	0.64	0.72
		WOA-FDD	1	0.56	0.76
5	2500 rpm, variable load	BA-FDD	2	0.88	0.77
		GWO-FDD	1	0.72	0.84
		WOA-FDD	1	0.65	0.88
6	3000 rpm, variable load	BA-FDD	1	0.95	0.86
		GWO-FDD	1	0.75	0.95
		WOA-FDD	1	0.60	0.96

TABLE 4 Simulation test results under variable load conditions

S. No	Operating conditions	Optimization techniques	Number of misclassifications	Maximum misclassification time (s)	Response time (s)
1	20% load, variable speed	BA-FDD	3	0.7	1.08
		GWO-FDD	3	0.75	1.16
		WOA-FDD	2	0.68	1.18
2	40% load, variable speed	BA-FDD	4	1.14	1.24
		GWO-FDD	2	1.05	1.24
		WOA-FDD	2	0.9	1.3
3	60% load, variable speed	BA-FDD	4	1.26	1.43
		GWO-FDD	3	1.13	1.49
		WOA-FDD	2	1.05	1.55
4	80% load, variable speed	BA-FDD	3	1.41	1.52
		GWO-FDD	3	1.26	1.6
		WOA-FDD	2	1.18	1.64
5	100% load, variable speed	BA-FDD	3	1.5	1.65
		GWO-FDD	2	1.34	1.72
		WOA-FDD	2	0.99	1.76

4.4 | Knowledge-based fault diagnosis

The knowledge-based method uses artificial intelligence (AI) techniques to achieve fault detection through machine learning, reasoning, and decision making, without the need for a mathematical model of the PM machine. BA, GWO,

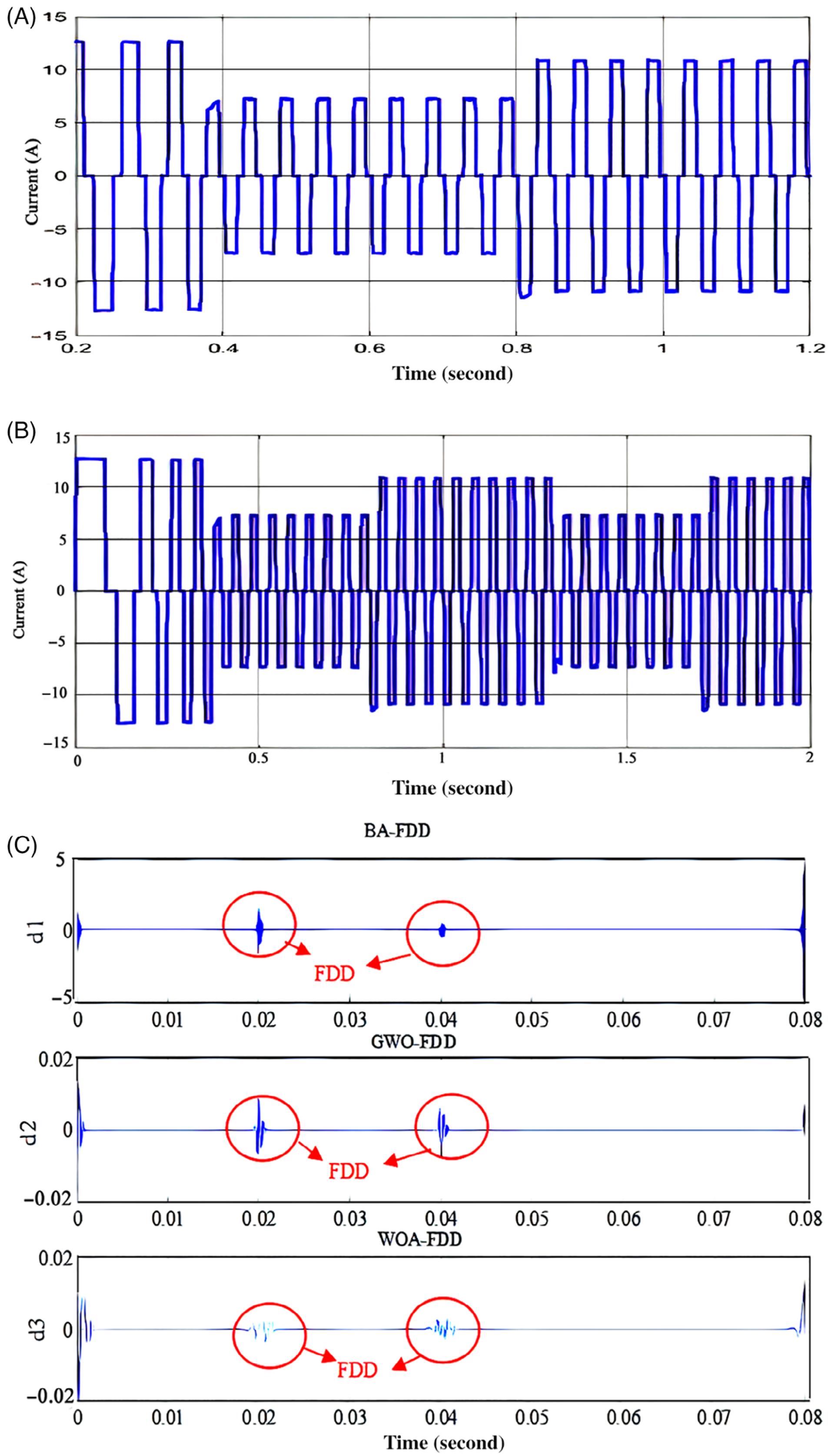

FIGURE 14 (A) WOA-based fault diagnosis for stator current in stator winding of BLDC motor. (B) WOA-based fault diagnosis for stator current in stator winding of BLDC motor. (C) BA-, GWO-, and WOA-based fault diagnosis for sensorless BLDC motor

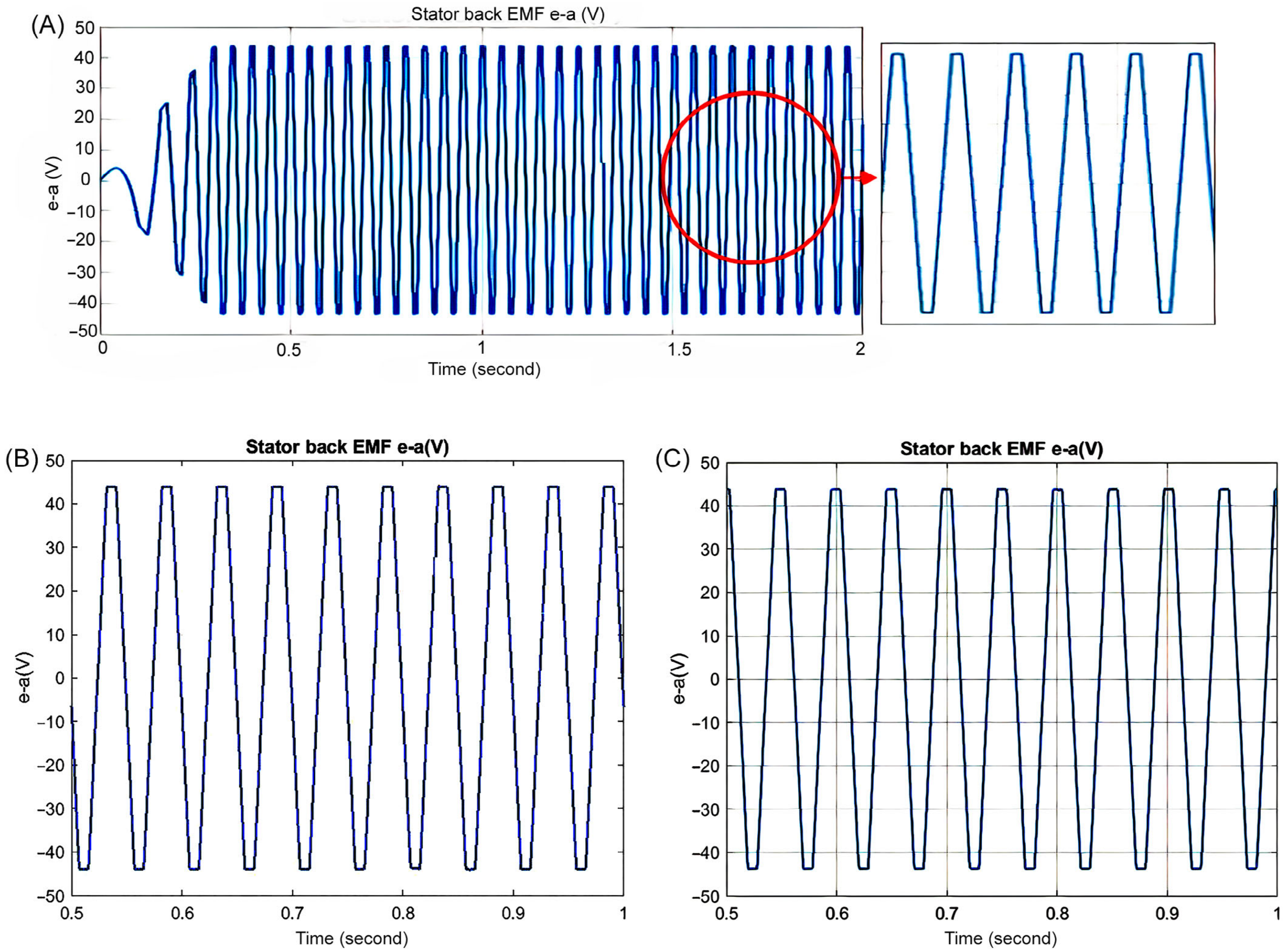

FIGURE 15 (a) WOA-based fault diagnosis for stator back EMF of BLDC motor. (B and C) WOA-based fault diagnosis for stator back EMF of BLDC motor

and WOA are some of the most often adopted. The representation of knowledge-based fault diagnosis is shown in Figure 11.

Deals with the BA, GWO, and WOA approached FDD for speed control of BLDC motor drive under varying load conditions, varying set speed conditions, and integrated conditions. The effectiveness of the BA-, GWO-, and WOA-based FDD MATLAB simulation results is analyzed.

5 | RESULTS AND DISCUSSION

This section provides MATLAB/Simulink simulation results of the FDD methods applied to a sensorless BLDC motor, for the bearing faults and the stator winding faults. In terms of bearings, previous studies show that 90% of faults that occur in rolling bearings are due to cracks in the inner and outer races.[29] Accordingly, four bearing conditions were considered in this study, namely the normal condition, the outer race fault, the inner race fault, and the presence of both the inner and outer race faults.[30] The vibration of the machine was measured, and optimization techniques were applied for the diagnosis of these faults. The parameters of the optimization algorithm are shown in Table 1.

The bearing and BLDC motor parameters are shown in Table 2. The evaluate the performance of FDD for sensorless BLDC motor using optimization techniques such as BA, GWO, and WOA in terms of different simulation setup. Those optimization techniques are used for the FDD in speed control of the BLDC motor. The proposed design is

TABLE 5 Accuracy of FDD in sensorless BLDC motor using optimization techniques

S.No	Operating conditions	Optimization techniques	Percentage of accuracy (%)			
			Principle component analysis	Empirical mode decomposition	Dynamic neural networks	Orthogonal fuzzy neighborhood discriminant analysis
1	1000 rpm	BA-FDD	86.5	89.5	91	92.5
		GWO-FDD	87.5	90.5	91.5	93.5
		WOA-FDD	87.5	91	93	94
2	2000 rpm	BA-FDD	85	88	91.5	93
		GWO-FDD	85	88.5	92.5	93.5
		WOA-FDD	86	90	93	95
3	3000 rpm	BA-FDD	85	89	94	94
		GWO-FDD	87	91.5	95	95.5
		WOA-FDD	88.5	91.5	93	96
4	No Load	BA-FDD	84	89	91	92.5
		GWO-FDD	84	89	93	93
		WOA-FDD	86	91	93	94.5
5	50% Load	BA-FDD	84	88	92	93
		GWO-FDD	85	89.5	92.5	93.5
		WOA-FDD	86	90	93	95
6	100% Load	BA-FDD	88	91	92	95
		GWO-FDD	88.5	91	93.5	96
		WOA-FDD	89.5	92	93.5	97

TABLE 6 Accuracy of bearing fault under various operating conditions

S.No	Operating conditions	Bearing faults	Percentage of accuracy in simulation test	Percentage of fault reduction
1	1000 rpm	Inner	98.60	6
		Outer	97.54	5
		Ball	96.23	6
2	2000 rpm	Inner	97.56	6
		Outer	96.11	5
		Ball	95.25	6
3	3000 rpm	Inner	96.47	5
		Outer	95.72	5
		Ball	95.12	6
4	No load	Inner	96.33	6
		Outer	97.52	5
		Ball	95.61	6
5	50% Load	Inner	96.23	5
		Outer	95.14	6
		Ball	95.06	7
6	100% Load	Inner	97.25	6
		Outer	96.45	7
		Ball	95.36	9

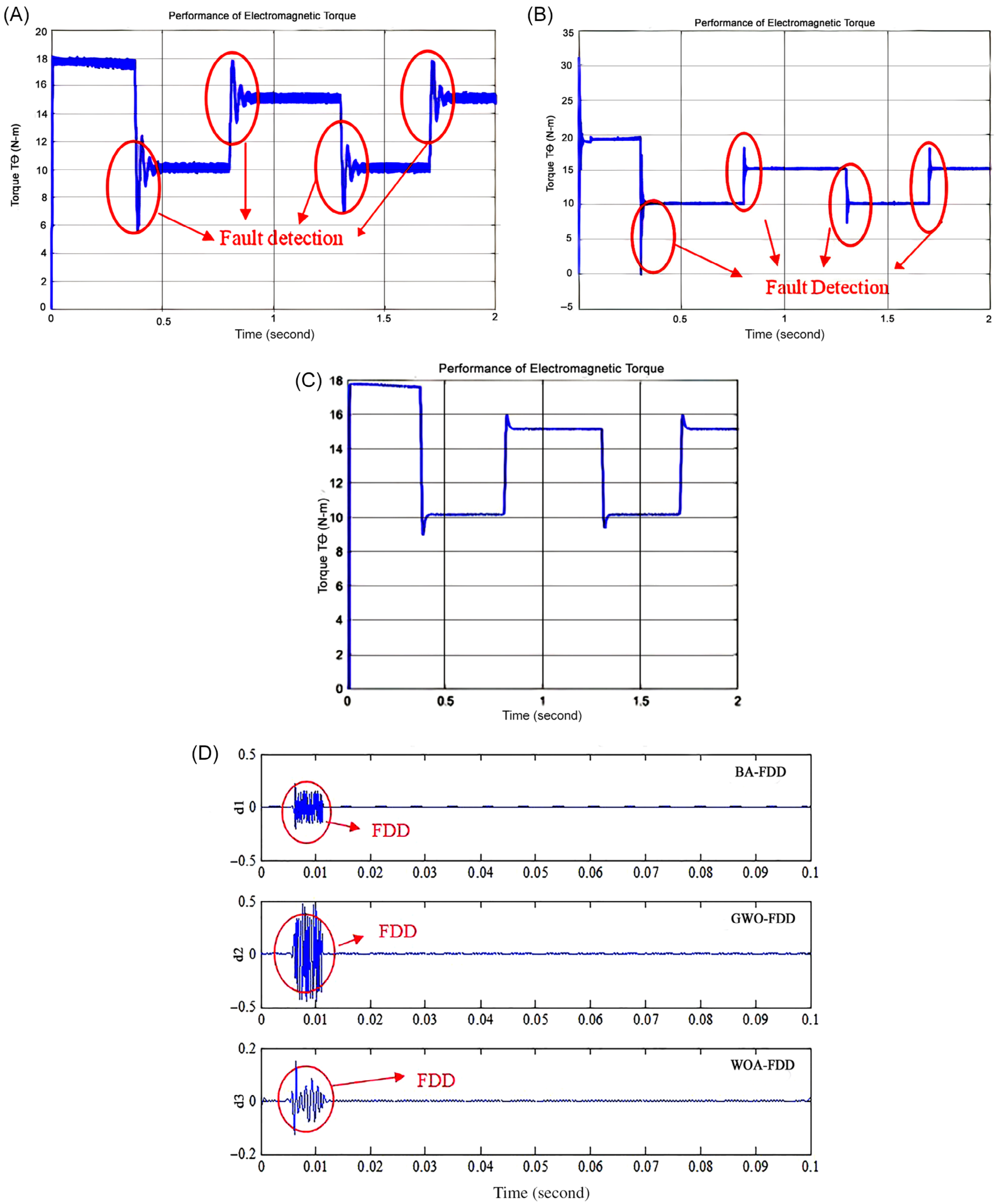

FIGURE 16 (A and B) Fault detection for electromagnetic torque of BLDC motor. (C) WOA-based fault diagnosis for electromagnetic torque of BLDC motor. (D) BA-, GWO-, and WOA-based FDD for sensorless BLDC motor

TABLE 7 Results of 10 consecutive fault diagnosis in the MATLAB simulations

		Accuracy of optimization techniques iteration (%)										
Operating conditions	**Optimization techniques**	**1**	**2**	**3**	**4**	**5**	**6**	**7**	**8**	**9**	**10**	**Average**
1000 rpm	BA-FDD	88.5	86.5	84.5	82.6	85.6	87.4	86.5	89.5	89.0	83.6	86.4
	GWO-FDD	88.6	89.4	87.6	92.5	96.5	94.8	92.8	93.4	95.6	91.4	92.3
	WOA-FDD	91.5	92.6	90.5	93.6	97.5	94.9	95.6	96.8	96.5	96.0	94.6
2000 rpm	BA-FDD	89.3	87.3	85.3	83.4	86.4	88.2	87.3	90.3	89.8	84.4	87.1
	GWO-FDD	89.3	90.2	88.3	93.3	97.3	95.6	93.6	94.2	96.4	92.2	93.0
	WOA-FDD	92.3	93.3	91.3	94.4	98.3	95.6	96.4	97.6	97.3	96.7	95.3
3000 rpm	BA-FDD	90.7	88.7	86.6	84.7	87.7	89.6	88.7	91.7	91.2	85.7	88.5
	GWO-FDD	90.8	91.6	89.7	94.8	98.9	97.2	95.1	95.7	98.0	93.7	94.6
	WOA-FDD	93.8	94.9	92.8	95.9	99.9	97.2	98.0	99.2	99.0	98.4	96.9
No Load	BA-FDD	88.5	86.5	84.5	82.6	85.6	87.4	86.5	89.5	89.0	83.6	86.4
	GWO-FDD	88.6	89.4	87.6	92.5	96.5	94.8	92.8	93.4	95.6	91.4	92.3
	WOA-FDD	91.5	92.6	90.5	93.6	97.5	94.9	95.6	96.8	96.5	96.0	94.6
50% Load	BA-FDD	90.7	88.7	86.6	84.7	87.7	89.6	88.7	91.7	91.2	85.7	88.5
	GWO-FDD	90.8	91.6	89.7	94.8	98.9	97.2	95.1	95.7	98.0	93.7	94.6
	WOA-FDD	93.8	94.9	92.8	95.9	99.9	97.2	98.0	99.2	99.0	98.4	96.9
100% Load	BA-FDD	92.0	90.0	87.9	85.9	89.0	90.9	90.0	93.1	92.6	86.9	89.8
	GWO-FDD	92.1	93.0	91.1	96.2	97.0	98.6	96.5	97.1	99.4	95.1	95.6
	WOA-FDD	95.2	96.3	94.2	97.3	96.5	98.6	97.0	97.3	97.6	99.8	97.0

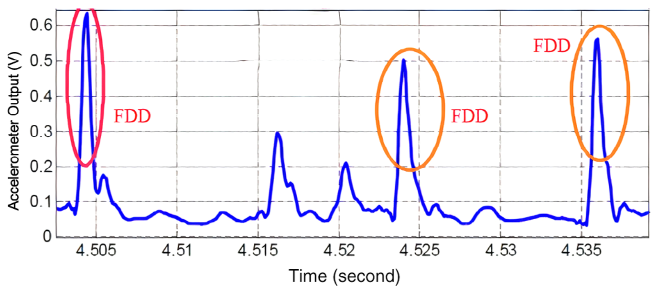

FIGURE 17 Simulated vibration signal from faulty bearing

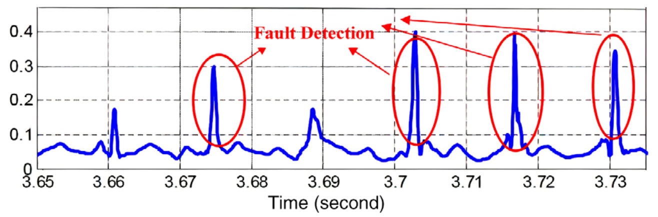

FIGURE 18 Simulated vibration signal from a faulty bearing

implemented using MATLAB/SIMULINK simulation tool. The performance of the proposed FDD methods is compared with the existing techniques in sensorless speed control of BLDC motor using BA, GWO, and WOA techniques. Figure 12 shows the three-phase current in the BLDC motor.

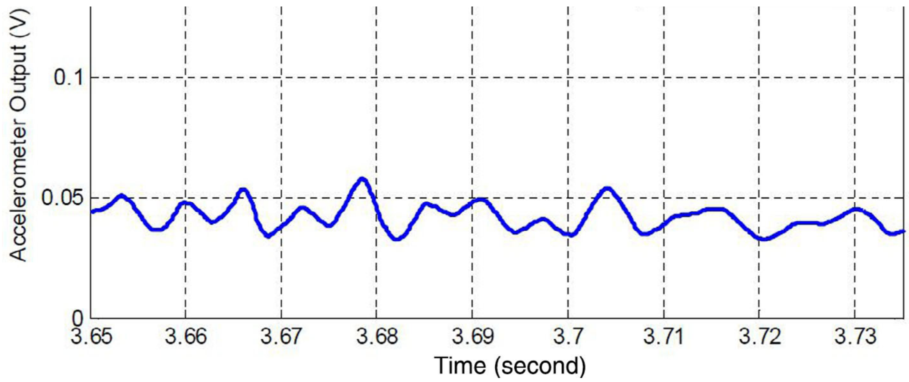

FIGURE 19 WOA-based fault diagnosis for vibration signal of BLDC motor

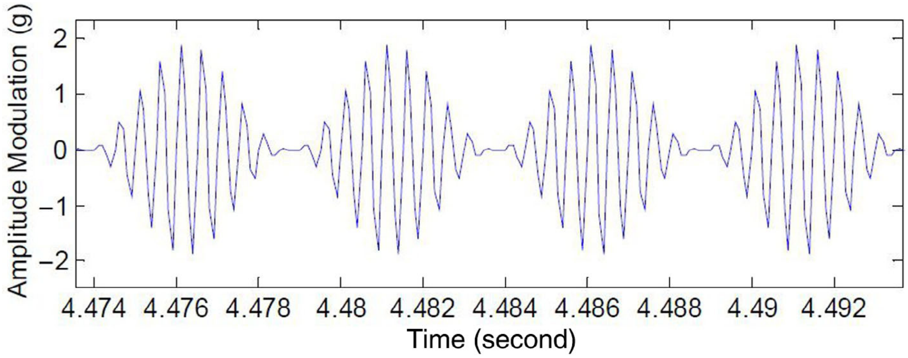

FIGURE 20 WOA-based fault diagnosis for amplitude modulation phenomenon

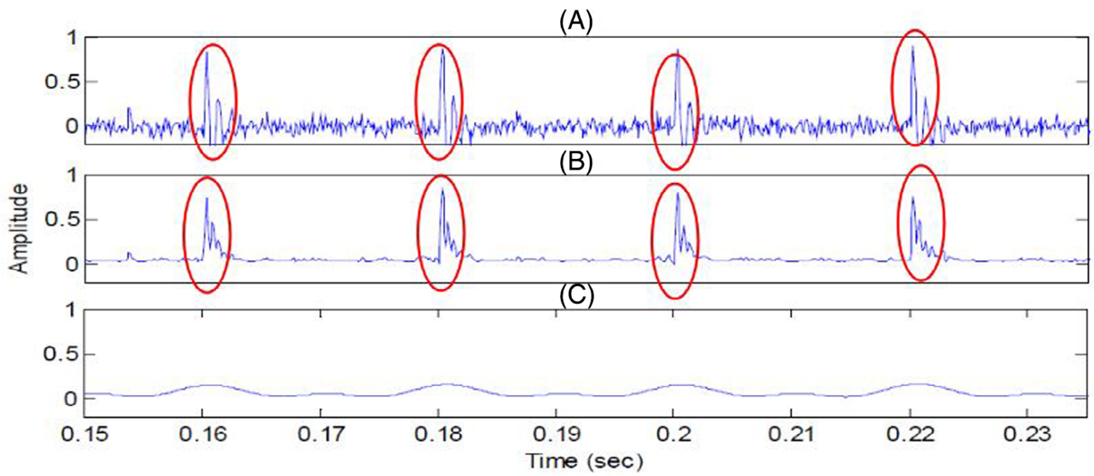

FIGURE 21 (A) Simulated vibration signal from a faulty bearing using BA, (B) denoised signal using GWO, and (C) denoised signal using WOA

5.1 | WOA-based FDD for stator current in stator winding of BLDC motor

Analyzing only the bearing fault of the BLDC motor is not sufficient to detect the variations in phase currents. Therefore, the BLDC motor stator current in stator winding is analyzed by FDD components using BA, GWO, and WOA. Figure 13A-D represents the fault detection for stator current in the stator winding of the BLDC motor.

Tables 3 and 4 show the simulation test results for the BLDC motor under variable speed and load situations, respectively. Forty percentage of each table dataset acquired from the simulation results was set aside for evaluating the

TABLE 8 Mean, standard deviation, and computation time

S.No	Operating conditions	Optimization techniques	Mean	SD	Computation time (s)
1	1000 rpm	BA-FDD	0.356582	0.45326	521.87
		GWO-FDD	0.350125	0.43876	512.53
		WOA-FDD	0.347352	0.37425	502.35
2	2000 rpm	BA-FDD	0.356215	0.44325	550.36
		GWO-FDD	0.354265	0.42354	536.68
		WOA-FDD	0.345684	0.40213	521.87
3	3000 rpm	BA-FDD	0.369322	0.47156	531.87
		GWO-FDD	0.360435	0.40155	512.53
		WOA-FDD	0.354153	0.37153	502.35
4	No Load	BA-FDD	0.369254	0.44256	5440.36
		GWO-FDD	0.361242	0.41356	536.68
		WOA-FDD	0.350124	0.38245	511.87
5	50% Load	BA-FDD	0.364258	0.42356	532.53
		GWO-FDD	0.371452	0.39564	512.35
		WOA-FDD	0.368452	0.37245	504.36
6	100% Load	BA-FDD	0.363108	0.39525	536.68
		GWO-FDD	0.370482	0.40885	526.36
		WOA-FDD	0.362586	0.37985	512.16

WOA-based FDD. A series of optimization from the healthy case was prefixed to the data acquired for each operating condition and BA, GWO, and WOA. From a faulty condition, the WOA-based diagnosis test for motors running at variable speed and maximum loading circumstances. The WOA based Fault Diagnosis for stator current in stator winding of BLDC motor is shown in Figure 14A-C.

5.2 | WOA-based FDD for bearing faults in BLDC motor drives

The WOA-based denoising scheme consists of three processes, namely vibration sensor, wavelet analysis, and fault identification. The core of this scheme is the vibration sensor and wavelet denoising process, where the input signal is firstly transformed into wavelet coefficients. Then, the wavelet coefficients using bivariate shrinkage to denoise the coefficients. Finally, the denoised coefficients are inversely transformed back to the time domain to obtain the denoised signal. In the following part of this section, the WOA-FDD results obtained using the aforementioned methods will be presented. The FDD results were obtained using the proposed WOA-based FDD for back EMF of the motor are shown in Figure 15A-C.

Under various operating conditions, the accuracy of FDD and bearing fault in sensorless BLDC motor using optimization techniques are shown in Tables 5 and 6, respectively. From the tables, it can be observed that the WOA-based FDD methods with a good percentage of accuracy score in the above qualitative analysis and minimum level of percentage of fault reduction under the above operating conditions.

The WOA-based fault diagnosis for electromagnetic torque of BLDC motor is shown in Figure 16A-C, and the results of 10 consecutive fault diagnoses in the MATLAB simulations are shown in Table 7. It is noted that WOA-based fault diagnosis is better iteration accuracy when compared to BA and GWO for speed control of BLDC motor under various operating conditions.

5.3 | Simulated vibration signal from a faulty bearing

A bearing contains a fault; the resulting vibration signal exhibits characteristic features that can be utilized to detect the fault. However, the vibration signal from a bearing with an incipient fault is usually masked by machine noise, making it difficult to detect the fault signature.

In this work, optimization techniques BA-, GWO-, and WOA-based FFD method for speed control of sensorless BLDC motor from the measured vibration signal. The simulated vibration signal from the faulty bearing is shown in Figures 17 and 18.

Figures 19 and 20 illustrate the WOA-based fault diagnosis for vibration signal of BLDC motor and amplitude modulation phenomenon. From the figures, it is noted that the faulty signal can be identified and denoised signal using WOA instantly under uncertain operating conditions. The simulated vibration signal from a faulty bearing using BA, GWO, and WOA is shown in Figure 21A-C.

In this research, bearing faults representing the mechanical elements of the motor and stator winding faults from the electrical elements of the motor were studied. For mechanical faults, further studies should involve applying the proposed methods on fault diagnosis of all components of the motor. In addition, the influence of the external load on

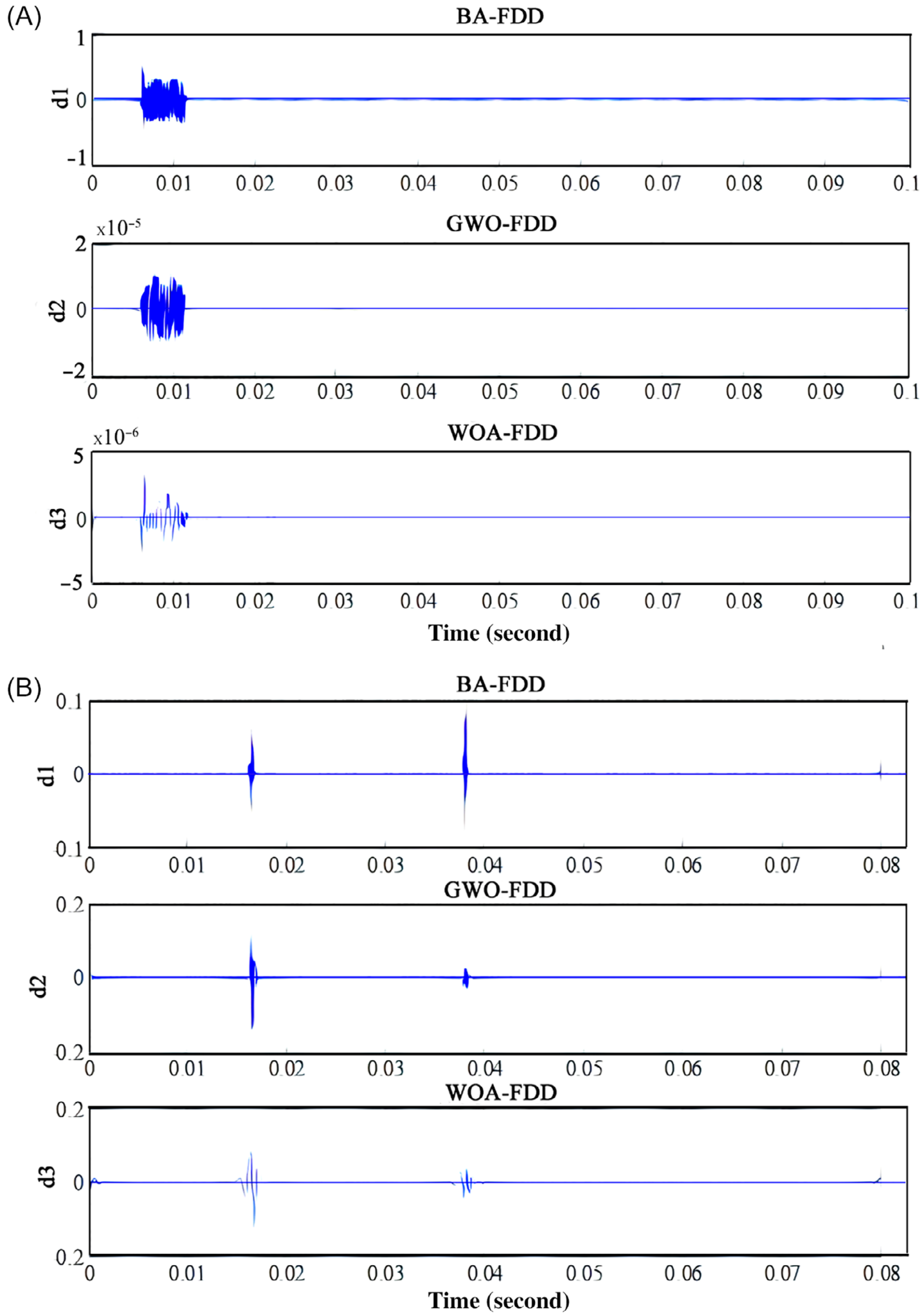

FIGURE 22 (A) BA-, GWO-, and WOA-based FDD for sensorless BLDC motor. (B) BA-, GWO-, and WOA-based FDD for sensorless BLDC motor

fault diagnosis should be investigated. In terms of parameter estimation of the motor, further studies should involve the implementation of other types of electric motors, such as induction and switched reluctance motors. The mean, SD, and computation time are shown in Table 8.

It is also suggested WOA-based FDD method has enhanced the sensorless-controlled BLDC motor drive's dependability by efficiently detecting, isolating, and compensating the problem in the bearing and stator winding under various operating conditions such as varying set speed conditions and varying load conditions. The BA-, GWO-, and WOA-based FDD for sensorless BLDC motor is shown in Figure 22A,B

5.4 | Recommendations and future work

In this work, bearing faults representing the mechanical elements of the motor and stator winding faults from the electrical elements of the motor were studied. For mechanical faults, further studies should involve applying the proposed methods on fault diagnosis of all components of the motor. In addition, the influence of the external load on fault diagnosis should be investigated. In terms of parameter estimation of the motor, further studies should involve the implementation of other types of electric motors, such as induction and switched reluctance motors.

For further work, the parameters for the BLDC motor should be acquired by conduct measurements on a real machine to get more precise values. The BLDC motor could be simulated with added noise to verify if the FDD method could still find the fault at nonideal conditions since that would more accurately represent a real machine. The FDD method should be tested on a real machine since the analytically modeled machine has estimated parameters and ideal conditions. This would be the most accurate way to validate the FDD method. The FDD method should lastly be implemented on a live machine to test if it works as intended. The experimental verification of speed control of sensorless BLDC motor could be an interesting base for a WOA-based FFD method and is suggested for further work.

6 | CONCLUSION

An efficient fault detection and diagnosis for speed control of sensorless BLDC motor drive using BA, GWO, and WOA are presented. It can be an improved the reliability, robustness speed control, and transient characteristics of industrial machinery. This work provided an overview of the mechanical faults and the electrical faults of BLDC motors, with a special focus on bearing and stator winding faults. In terms of bearing faults, vibration-based techniques are the most reliable. To enhance the characteristic features of a fault, the optimization techniques BA-, GWO-, and WOA-based FDD have been proposed. Among them, the wavelet analysis has shown its superiority in signal denoising and feature extraction. In terms of stator winding faults, the model-based parameter estimation techniques were found to be most promising.

From the simulation results, it is concluded that WOA-based FDD methods with a good percentage of accuracy score in the various qualitative analysis, quick response time, and high accuracy of optimization techniques iteration in percentage uses in the speed control of sensorless BLDC motor under uncertain operating conditions.

PEER REVIEW
The peer review history for this article is available at https://publons.com/publon/10.1002/2050-7038.13251.

DATA AVAILABILITY STATEMENT
Data sharing is not applicable to this article as no new data were created or analyzed in this study.

ORCID
Kumarasamy Vanchinathan https://orcid.org/0000-0003-1931-685X
KarumanchettyThottam Ramasamy Valluvan https://orcid.org/0000-0003-0298-4640
Chinnaraj Gnanavel https://orcid.org/0000-0002-5715-1753
Chandrasekaran Gokul https://orcid.org/0000-0002-3569-9443
Johny Renoald Albert https://orcid.org/0000-0002-4956-5999

REFERENCES

1. Abed W, Sharma S, Sutton R, Motwani A. A robust bearing fault detection and diagnosis technique for brushless DC motors under non-stationary operating conditions. *J Control Autom Electr Syst*. 2015;26(3):241-254.
2. Isermann R. Model-based fault-detection and diagnosis–status and applications. *Annu Rev Control*. 2005;29(1):71-85.
3. Moseler O, Isermann R. Application of model-based fault detection to a brushless DC motor. *IEEE Trans Ind Electron*. 2000;47(5):1015-1020.
4. Vanchinathan K, Valluvan KR. A metaheuristic optimization approach for tuning of fractional-order PID controller for speed control of sensorless BLDC motor. *J Circuits Syst Comput*. 2018;27(8):1850123-1–1850123-19.
5. Ebadpour M, Amiri N, Jatskevich J. Fast fault-tolerant control for improved dynamic performance of hall-sensor-controlled brushless DC motor drives. *IEEE Trans Power Electron*. 2021;36:14051–14061.
6. Mousmi A, Abbou A, El Houm Y. Binary diagnosis of hall effect sensors in brushless DC motor drives. *IEEE Trans Power Electron*. 2019;35(4):3859-3868.
7. Jafari A, Faiz J, Jarrahi MA. A simple and efficient current-based method for Interturn fault detection in BLDC motors. *IEEE Trans Ind Inform*. 2020;17(4):2707-2715.
8. Wang H, Lu S, Qian G, Ding J, Liu Y, Wang Q. A two-step strategy for online fault detection of high-resistance connection in BLDC motor. *IEEE Trans Power Electron*. 2019;35(3):3043-3053.
9. Vanchinathan K, Valluvan KR. Tuning of fractional order proportional integral derivative controller for speed control of sensorless BLDC motor using artificial bee Colony optimization technique. *Intelligent and Efficient Electrical Systems*. Singapore: Springer; 2018:117-127.
10. Medeiros RL, Lima Filho AC, Ramos JGG, Nascimento TP, Brito AV. A novel approach for speed and failure detection in brushless DC motors based on chaos. *IEEE Trans Ind Electron*. 2018;66(11):8751-8759.
11. Zhang Q, Feng M. Fast fault diagnosis method for hall sensors in brushless dc motor drives. *IEEE Trans Power Electron*. 2018;34(3):2585-2596.
12. Cai J, Zhao X. Synthetic hybrid-integral-threshold logic-based position fault diagnosis scheme for SRM drives. *IEEE Trans Instrum Meas*. 2020;70:1-8.
13. Rajasekaran P, Vanchinathan K. Improved performance of four switches three-phase brushless dc motor using speed-current control algorithm. *Int J Comput Appl*. 2013;68(11):1-7.
14. Arafat AKM, Choi S, Baek J. Open-phase fault detection of a five-phase permanent magnet assisted synchronous reluctance motor based on symmetrical components theory. *IEEE Trans Ind Electron*. 2017;64(8):6465-6474.
15. Munikoti S, Das L, Natarajan B, Srinivasan B. Data-driven approaches for diagnosis of incipient faults in dc motors. *IEEE Trans Ind Inform*. 2019;15(9):5299-5308.
16. Lu S, Wang X. A new methodology to estimate the rotating phase of a BLDC motor with its application in variable-speed bearing fault diagnosis. *IEEE Trans Power Electron*. 2017;33(4):3399-3410.
17. Vanchinathan K, Valluvan KR. A study of sensorless BLDC motor drives and future trends. *Asian J Res Soc Sci Humanit*. 2016;6(9):1863-1887.
18. Choi S, Haque MS, Tarek MTB, et al. Fault diagnosis techniques for permanent magnet AC machine and drives—a review of the current state of the art. *IEEE Trans Transport Electrif*. 2018;4(2):444-463.
19. Lu S, Qin Y, Hang J, Zhang B, Wang Q. Adaptively estimating rotation speed from DC motor current ripple for order tracking and fault diagnosis. *IEEE Trans Instrum Meas*. 2018;68(3):741-753.
20. Duran MJ, Gonzalez-Prieto I, Rios-Garcia N, Barrero F. A simple, fast, and robust open-phase fault detection technique for six-phase induction motor drives. *IEEE Trans Power Electron*. 2017;33(1):547-557.
21. Chandrasekaran G, Kumarasamy V, Chinraj G. Test scheduling of core based system-on-chip using modified ant colony optimization. *J Eur Syst Autom*. 2019;52(6):599-605.
22. Alshorman O, Alshorman A. A review of intelligent methods for condition monitoring and fault diagnosis of stator and rotor faults of induction machines. *Int J Electr Comput Eng*. 2021;11(4):2820-2829.
23. Vanchinathan K, Selvaganesan N. Adaptive fractional order PID controller tuning for brushless DC motor using artificial bee colony algorithm. *Res Control Optim*. 2021;4:100032. https://doi.org/10.1016/j.rico.2021.100032
24. Chandrasekaran G, Karthikeyan PR, Kumar NS, Kumarasamy V. Test scheduling of system-on-chip using dragonfly and ant lion optimization algorithms. *J Intell Fuzzy Syst*. 2021;40(3):4905-4917.
25. Liu XQ, Zhang HY, Liu J, Yang J. Fault detection and diagnosis of permanent-magnet DC motor based on parameter estimation and neural network. *IEEE Trans Ind Electron*. 2000;47(5):1021-1030.
26. Yin B, Wang C, Abza F. New brain tumor classification method based on an improved version of whale optimization algorithm. *Biomed Signal Process Control*. 2020;56:101728.
27. Kumarasamy V, Ramasamy VK, Chinnaraj G. Systematic design of multi-objective enhanced genetic algorithm optimized fractional order PID controller for sensorless brushless DC motor drive. *Circuit World*. 2021. https://doi.org/10.1108/CW-07-2020-0137
28. Wang H, Wu F, Zhang L. Application of variational mode decomposition optimized with improved whale optimization algorithm in bearing failure diagnosis. *Alex Eng J*. 2021;60(5):4689-4699.

29. Vanchinathan K, Valluvan KR, Gnanavel C, Gokul C. Design methodology and experimental verification of intelligent speed controllers for sensorless permanent magnet brushless DC motor: intelligent speed controllers for electric motor. *Int Trans Electr Energy Syst*. 2021; 31(9):1-20.
30. Vanchinathan K, Sathiskumar P, Selvaganesan N. A Metaheuristic Optimization Algorithm-Based Speed Controller for Brushless DC Motor: Industrial Case Study. *Metaheuristic Algorithms in Industry 4.0*. CRC Press; 2021:189-216.

How to cite this article: Vanchinathan K, Valluvan KR, Gnanavel C, Gokul C, Albert JR. An improved incipient whale optimization algorithm based robust fault detection and diagnosis for sensorless brushless DC motor drive under external disturbances. *Int Trans Electr Energ Syst*. 2021;31(12):e13251. doi:10.1002/2050-7038.13251